Beam energy dependence of rapidity-even dipolar flow in Au+Au collisions

STAR Collaboration

J. Adam [i], L. Adamczyk [a], J.R. Adams [ae], J.K. Adkins [u], G. Agakishiev [s], M.M. Aggarwal [ag], Z. Ahammed [bd], N.N. Ajitanand [ar], I. Alekseev [q,ab], D.M. Anderson [at], R. Aoyama [ax], A. Aparin [s], D. Arkhipkin [c], E.C. Aschenauer [c], M.U. Ashraf [aw], F. Atetalla [t], A. Attri [ag], G.S. Averichev [s], X. Bai [g], V. Bairathi [ac], K. Barish [az], A.J. Bassill [az], A. Behera [ar], R. Bellwied [av], A. Bhasin [r], A.K. Bhati [ag], J. Bielcik [j], J. Bielcikova [k], L.C. Bland [c], I.G. Bordyuzhin [q], J.D. Brandenburg [al], A.V. Brandin [ab], D. Brown [y], J. Bryslawskyj [az], I. Bunzarov [s], J. Butterworth [al], H. Caines [bg], M. Calderón de la Barca Sánchez [e], J.M. Campbell [ae], D. Cebra [e], I. Chakaberia [t,ap], P. Chaloupka [j], F.-H. Chang [ad], Z. Chang [c], N. Chankova-Bunzarova [s], A. Chatterjee [bd], S. Chattopadhyay [bd], J.H. Chen [aq], X. Chen [ao], X. Chen [w], J. Cheng [aw], M. Cherney [i], W. Christie [c], G. Contin [x], H.J. Crawford [d], S. Das [g], T.G. Dedovich [s], I.M. Deppner [ba], A.A. Derevschikov [ai], L. Didenko [c], C. Dilks [ah], X. Dong [x], J.L. Drachenberg [v], J.C. Dunlop [c], L.G. Efimov [s], N. Elsey [bf], J. Engelage [d], G. Eppley [al], R. Esha [f], S. Esumi [ax], O. Evdokimov [h], J. Ewigleben [y], O. Eyser [c], R. Fatemi [u], S. Fazio [c], P. Federic [k], P. Federicova [j], J. Fedorisin [s], P. Filip [s], E. Finch [ay], Y. Fisyak [c], C.E. Flores [e], L. Fulek [a], C.A. Gagliardi [at], T. Galatyuk [l], F. Geurts [al], A. Gibson [bc], D. Grosnick [bc], D.S. Gunarathne [as], Y. Guo [t], A. Gupta [r], W. Guryn [c], A.I. Hamad [t], A. Hamed [at], A. Harlenderova [j], J.W. Harris [bg], L. He [aj], S. Heppelmann [ah], S. Heppelmann [e], N. Herrmann [ba], A. Hirsch [aj], L. Holub [j], S. Horvat [bg], X. Huang [aw], B. Huang [h], S.L. Huang [ar], H.Z. Huang [f], T. Huang [ad], T.J. Humanic [ae], P. Huo [ar], G. Igo [f], W.W. Jacobs [p], A. Jentsch [au], J. Jia [c,ar], K. Jiang [ao], S. Jowzaee [bf], E.G. Judd [d], S. Kabana [t], D. Kalinkin [p], K. Kang [aw], D. Kapukchyan [az], K. Kauder [bf], H.W. Ke [c], D. Keane [t], A. Kechechyan [s], D.P. Kikoła [be], C. Kim [az], T.A. Kinghorn [e], I. Kisel [m], A. Kisiel [be], L. Kochenda [ab], L.K. Kosarzewski [be], A.F. Kraishan [as], L. Kramarik [j], L. Krauth [az], P. Kravtsov [ab], K. Krueger [b], N. Kulathunga [av], S. Kumar [ag], L. Kumar [ag], J. Kvapil [j], J.H. Kwasizur [p], R. Lacey [ar,*], J.M. Landgraf [c], J. Lauret [c], A. Lebedev [c], R. Lednicky [s], J.H. Lee [c], X. Li [ao], C. Li [ao], W. Li [aq], Y. Li [aw], Y. Liang [t], J. Lidrych [j], T. Lin [at], A. Lipiec [be], M.A. Lisa [ae], F. Liu [g], P. Liu [ar], H. Liu [p], Y. Liu [at], T. Ljubicic [c], W.J. Llope [bf], M. Lomnitz [x], R.S. Longacre [c], X. Luo [g], S. Luo [h], G.L. Ma [aq], Y.G. Ma [aq], L. Ma [n], R. Ma [c], N. Magdy [ar], R. Majka [bg], D. Mallick [ac], S. Margetis [t], C. Markert [au], H.S. Matis [x], O. Matonoha [j], D. Mayes [az], J.A. Mazer [am], K. Meehan [e], J.C. Mei [ap], N.G. Minaev [ai], S. Mioduszewski [at], D. Mishra [ac], B. Mohanty [ac], M.M. Mondal [o], I. Mooney [bf], D.A. Morozov [ai], Md. Nasim [f], J.D. Negrete [az], J.M. Nelson [d], D.B. Nemes [bg], M. Nie [aq], G. Nigmatkulov [ab], T. Niida [bf], L.V. Nogach [ai], T. Nonaka [ax], S.B. Nurushev [ai], G. Odyniec [x], A. Ogawa [c], K. Oh [ak], S. Oh [bg], V.A. Okorokov [ab], D. Olvitt Jr. [as], B.S. Page [c], R. Pak [c],

* Corresponding author.

E-mail address: Roy.Lacey@Stonybrook.edu (R. Lacey).

Y. Panebratsev [s], B. Pawlik [af], H. Pei [g], C. Perkins [d], J. Pluta [be], J. Porter [x], M. Posik [as],
N.K. Pruthi [ag], M. Przybycien [a], J. Putschke [bf], A. Quintero [as], S.K. Radhakrishnan [x],
S. Ramachandran [u], R.L. Ray [au], R. Reed [y], H.G. Ritter [x], J.B. Roberts [al], O.V. Rogachevskiy [s],
J.L. Romero [e], L. Ruan [c], J. Rusnak [k], O. Rusnakova [j], N.R. Sahoo [at], P.K. Sahu [o], S. Salur [am],
J. Sandweiss [bg], J. Schambach [au], A.M. Schmah [x], W.B. Schmidke [c], N. Schmitz [z],
B.R. Schweid [ar], F. Seck [l], J. Seger [i], M. Sergeeva [f], R. Seto [az], P. Seyboth [z], N. Shah [aq],
E. Shahaliev [s], P.V. Shanmuganathan [y], M. Shao [ao], W.Q. Shen [aq], F. Shen [ap], S.S. Shi [g],
Q.Y. Shou [aq], E.P. Sichtermann [x], S. Siejka [be], R. Sikora [a], M. Simko [k], S. Singha [t],
N. Smirnov [bg], D. Smirnov [c], W. Solyst [p], P. Sorensen [c], H.M. Spinka [b], B. Srivastava [aj],
T.D.S. Stanislaus [bc], D.J. Stewart [bg], M. Strikhanov [ab], B. Stringfellow [aj], A.A.P. Suaide [an],
T. Sugiura [ax], M. Sumbera [k], B. Summa [ah], Y. Sun [ao], X. Sun [g], X.M. Sun [g], B. Surrow [as],
D.N. Svirida [q], P. Szymanski [be], Z. Tang [ao], A.H. Tang [c], A. Taranenko [ab], T. Tarnowsky [aa],
J.H. Thomas [x], A.R. Timmins [av], D. Tlusty [al], T. Todoroki [c], M. Tokarev [s], C.A. Tomkiel [y],
S. Trentalange [f], R.E. Tribble [at], P. Tribedy [c], S.K. Tripathy [o], O.D. Tsai [f], B. Tu [g], T. Ullrich [c],
D.G. Underwood [b], I. Upsal [ae], G. Van Buren [c], J. Vanek [k], A.N. Vasiliev [ai], I. Vassiliev [m],
F. Videbæk [c], S. Vokal [s], S.A. Voloshin [bf], A. Vossen [p], G. Wang [f], Y. Wang [g], F. Wang [aj],
Y. Wang [aw], J.C. Webb [c], L. Wen [f], G.D. Westfall [aa], H. Wieman [x], S.W. Wissink [p], R. Witt [bb],
Y. Wu [t], Z.G. Xiao [aw], G. Xie [h], W. Xie [aj], Q.H. Xu [ap], Z. Xu [c], J. Xu [g], Y.F. Xu [aq], N. Xu [x],
S. Yang [c], C. Yang [ap], Q. Yang [ap], Y. Yang [ad], Z. Ye [h], Z. Ye [h], L. Yi [ap], K. Yip [c], I.-K. Yoo [ak],
N. Yu [g], H. Zbroszczyk [be], W. Zha [ao], Z. Zhang [aq], L. Zhang [g], Y. Zhang [ao], X.P. Zhang [aw],
J. Zhang [w], S. Zhang [aq], S. Zhang [ao], J. Zhang [x], J. Zhao [aj], C. Zhong [aq], C. Zhou [aq], L. Zhou [ao],
Z. Zhu [ap], X. Zhu [aw], M. Zyzak [m]

[a] AGH University of Science and Technology, FPACS, Cracow 30-059, Poland
[b] Argonne National Laboratory, Argonne, IL 60439
[c] Brookhaven National Laboratory, Upton, NY 11973
[d] University of California, Berkeley, CA 94720
[e] University of California, Davis, CA 95616
[f] University of California, Los Angeles, CA 90095
[g] Central China Normal University, Wuhan, Hubei 430079
[h] University of Illinois at Chicago, Chicago, IL 60607
[i] Creighton University, Omaha, NE 68178
[j] Czech Technical University in Prague, FNSPE, Prague, 115 19, Czech Republic
[k] Nuclear Physics Institute AS CR, Prague 250 68, Czech Republic
[l] Technische Universitat, Darmstadt, Germany
[m] Frankfurt Institute for Advanced Studies FIAS, Frankfurt 60438, Germany
[n] Fudan University, Shanghai, 200433, China
[o] Institute of Physics, Bhubaneswar 751005, India
[p] Indiana University, Bloomington, IN 47408
[q] Alikhanov Institute for Theoretical and Experimental Physics, Moscow 117218, Russia
[r] University of Jammu, Jammu 180001, India
[s] Joint Institute for Nuclear Research, Dubna, 141 980, Russia
[t] Kent State University, Kent, OH 44242
[u] University of Kentucky, Lexington, KY 40506-0055
[v] Lamar University, Physics Department, Beaumont, TX 77710
[w] Institute of Modern Physics, Chinese Academy of Sciences, Lanzhou, Gansu 730000
[x] Lawrence Berkeley National Laboratory, Berkeley, CA 94720
[y] Lehigh University, Bethlehem, PA 18015
[z] Max-Planck-Institut fur Physik, Munich 80805, Germany
[aa] Michigan State University, East Lansing, MI 48824
[ab] National Research Nuclear University MEPhI, Moscow 115409, Russia
[ac] National Institute of Science Education and Research, HBNI, Jatni 752050, India
[ad] National Cheng Kung University, Tainan 70101
[ae] Ohio State University, Columbus, OH 43210
[af] Institute of Nuclear Physics PAN, Cracow 31-342, Poland
[ag] Panjab University, Chandigarh 160014, India
[ah] Pennsylvania State University, University Park, PA 16802
[ai] Institute of High Energy Physics, Protvino 142281, Russia
[aj] Purdue University, West Lafayette, IN 47907
[ak] Pusan National University, Pusan 46241, Republic of Korea
[al] Rice University, Houston, TX 77251
[am] Rutgers University, Piscataway, NJ 08854
[an] Universidade de Sao Paulo, Sao Paulo, 05314-970, Brazil
[ao] University of Science and Technology of China, Hefei, Anhui 230026
[ap] Shandong University, Jinan, Shandong 250100
[aq] Shanghai Institute of Applied Physics, Chinese Academy of Sciences, Shanghai 201800
[ar] State University of New York, Stony Brook, NY 11794
[as] Temple University, Philadelphia, PA 19122

at *Texas A&M University, College Station, TX 77843*
au *University of Texas, Austin, TX 78712*
av *University of Houston, Houston, TX 77204*
aw *Tsinghua University, Beijing 100084*
ax *University of Tsukuba, Tsukuba, Ibaraki 305-8571, Japan*
ay *Southern Connecticut State University, New Haven, CT 06515*
az *University of California, Riverside, CA 92521*
ba *University of Heidelberg, Heidelberg, 69120, Germany*
bb *United States Naval Academy, Annapolis, MD 21402*
bc *Valparaiso University, Valparaiso, IN 46383*
bd *Variable Energy Cyclotron Centre, Kolkata 700064, India*
be *Warsaw University of Technology, Warsaw 00-661, Poland*
bf *Wayne State University, Detroit, MI 48201*
bg *Yale University, New Haven, CT 06520*

ARTICLE INFO

ABSTRACT

New measurements of directed flow for charged hadrons, characterized by the Fourier coefficient v_1, are presented for transverse momenta p_T, and centrality intervals in Au+Au collisions recorded by the STAR experiment for the center-of-mass energy range $\sqrt{s_{NN}} = 7.7$–200 GeV. The measurements underscore the importance of momentum conservation, and the characteristic dependencies on $\sqrt{s_{NN}}$, centrality and p_T are consistent with the expectations of geometric fluctuations generated in the initial stages of the collision, acting in concert with a hydrodynamic-like expansion. The centrality and p_T dependencies of v_1^{even}, as well as an observed similarity between its excitation function and that for v_3, could serve as constraints for initial-state models. The v_1^{even} excitation function could also provide an important supplement to the flow measurements employed for precision extraction of the temperature dependence of the specific shear viscosity.

High-energy nuclear collisions at the Relativistic Heavy Ion Collider (RHIC) and the Large Hadron Collider (LHC) can result in the creation of a plasma composed of strongly coupled quarks and gluons (QGP). Full characterization of this hot and dense matter is a major goal of present-day high-energy physics research. Recent studies have emphasized the use of anisotropic flow measurements to study the transport properties of this matter [1–9]. A current focus is centered on delineating the role of initial-state fluctuations, as well as reducing their influence on the uncertainties associated with the extraction of the temperature dependent specific shear viscosity (i.e. the ratio of shear viscosity to entropy density $\frac{\eta}{s}$(T)) of the QGP produced in these collisions [4–14].

The v_n coefficients used to characterize anisotropic flow, are normally obtained from a Fourier expansion of the azimuthal angle (ϕ) distribution of the particles produced orthogonal to the beam direction [15,16]:

$$\frac{dN}{d\phi} \propto 1 + 2 \sum_{n=1}^{\infty} v_n \cos n(\phi - \Psi_n), \tag{1}$$

where Ψ_n represents the nth order event plane, i.e., $\langle e^{in\phi} \rangle = v_n e^{in\Psi_n}$ and the brackets indicate averaging over particles and events. The coefficient v_1 is commonly termed directed flow, v_2 is the elliptic flow, v_3 is the triangular flow etc. For flow dominated distributions, the v_n coefficients are related to the Fourier coefficients v_{nn} used to characterize two-particle correlations in relative azimuthal angle $\Delta\phi = \phi_a - \phi_b$ for particle pairs a, b [17]:

$$\frac{dN^{pairs}}{d\Delta\phi} \propto 1 + 2 \sum_{n=1}^{\infty} v_{nn} \cos(n\Delta\phi). \tag{2}$$

However, so-called non-flow (NF) correlations can also contribute to the two-particle correlations [17–21]:

$$v_{nn}(p_T{}^a, p_T{}^b) = v_n(p_T{}^a) v_n(p_T{}^b) + \delta_{NF}, \tag{3}$$

where δ_{NF} includes possible contributions from resonance decays, Bose–Einstein correlations, jets, and global momentum conservation (GMC).

In the absence of fluctuations, the directed flow v_1 develops along the direction of the impact parameter [22] and is an odd function, $v_1^{odd}(\eta) = -v_1^{odd}(-\eta)$, of pseudorapidity. However, initial-state fluctuations, acting in concert with hydrodynamic-like expansion, gives an additional rapidity-even, $v_1^{even}(\eta) = v_1^{even}(-\eta)$, component [19,23] resulting in the total:

$$v_1(\eta) = v_1^{even}(\eta) + v_1^{odd}(\eta). \tag{4}$$

The magnitude of $v_1^{odd}(\eta)$ can be made negligible via a symmetric pseudorapidity selection, to give a straightforward measurement of $v_1^{even}(\eta)$.

The rapidity-even v_1 is proportional to the fluctuations-driven dipole asymmetry ε_1 of the system [19,23,24]; $v_1^{even} \propto \varepsilon_1$, where $\varepsilon_1 \equiv \langle |r^3 e^{i\phi}| \rangle / \langle r^3 \rangle$ and averaging is taken over the initial energy density after re-centering the coordinate system, i.e., $\langle |re^{i\phi}| \rangle = 0$. Hydrodynamical model calculations [20] indicate that the magnitude of v_1^{even} is sensitive to η/s, albeit with less sensitivity than for the higher order harmonics, $n \geq 2$. It has not been experimentally established whether this sensitivity depends on the temperature T, baryon chemical potential μ_B or both. Similarly it has not been established whether this sensitivity could reflect the influence of a possible critical end point (CEP) in the phase diagram for nuclear matter [25]. Therefore, differential v_1^{even} measurements that span a broad range of $\sqrt{s_{NN}}$ (T and μ_B), could potentially provide (i) unique supplemental constraints to discern between different initial-state models, (ii) aid precision extraction of η/s and study its possible dependence on T and μ_B, and (iii) give insight on the CEP. It is noteworthy that the paucity of v_1^{even} measurements at RHIC energies precludes their current use as constraints.

The present work employs two-particle correlation functions to extract $v_{11} = \langle \cos \Delta\phi \rangle$ values as a function of $p_T{}^a$, $p_T{}^b$ and centrality for a broad selection of beam energies. In turn the GMC
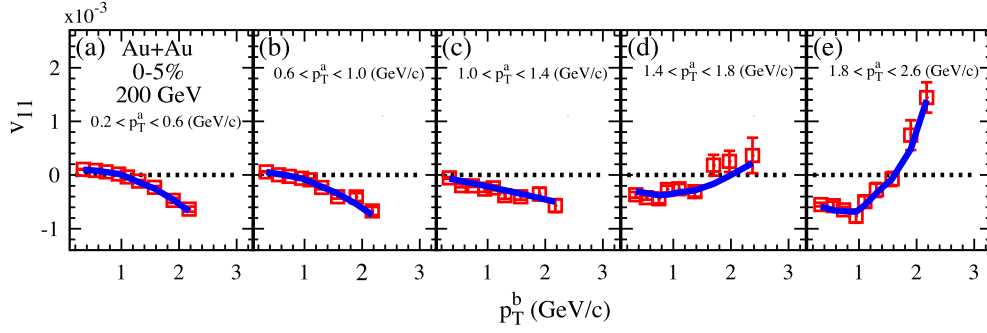
Fig. 1. v_{11} vs. p_T^b for several selections of p_T^a for 0–5% central Au+Au collisions at $\sqrt{s_{NN}} = 200$ GeV. The curve shows the result of the simultaneous fit with Eq. (7). The fit resulted in the value $\chi^2 = 1.1$ per degree of freedom (see text).

ansatz [18,26] is used in conjunction with the two-component fitting procedure outlined in Refs. [20,21] and discussed below, to extract v_1^{even} as a function of p_T and centrality for each value of $\sqrt{s_{NN}}$. The measurements indicate the characteristic p_T-dependent directed flow patterns associated with rapidity-even dipolar flow [19,23,24], as well as striking centrality and $\sqrt{s_{NN}}$ dependencies which could serve as constraints for initial- and final-state model inputs.

The data reported in this analysis are from Au+Au collisions spanning the full range of energies, $\sqrt{s_{NN}} = 7.7$–200 GeV, in beam energy scan I (BES-I), collected with the STAR detector using a minimum bias trigger. The collision vertices were reconstructed using charged-particle tracks measured in the Time Projection Chamber (TPC) [27]. The TPC covers the full azimuth and has a pseudo-rapidity range of $|\eta| < 1.0$. Events were selected to have a vertex position about the nominal center of the TPC (in the beam direction) of ± 30 cm at $\sqrt{s_{NN}} = 200$ GeV, ± 40 cm at $\sqrt{s_{NN}} = 62, 39, 27, 19.6$ and 14.5 GeV, ± 50 cm at $\sqrt{s_{NN}} = 11.5$ GeV and ± 70 cm at $\sqrt{s_{NN}} = 7.7$ GeV, and to be within a radius of 1–2 cm with respect to the beam axis. Note that the distribution of the vertex positions broadens (in the beam direction) as the beam energy is lowered.

The centrality of each collision was determined by measuring event-by-event multiplicity and interpreting the measurement with a tuned Monte Carlo Glauber calculation [28,29]. Analyzed tracks were required to have a distance of closest approach to the primary vertex to be less than 3 cm, and to have at least 15 TPC space points used in their reconstruction. Furthermore, the ratio of the number of fit points to the maximum possible number of TPC space points was required to be larger than 0.52 to remove split tracks. The p_T of tracks was limited to the range $0.2 < p_T < 4$ GeV/c.

The correlation function technique [17] was used to generate the two-particle $\Delta\phi$ correlations,

$$C_r(\Delta\phi, \Delta\eta) = \frac{(dN/d\Delta\phi)_{same}}{(dN/d\Delta\phi)_{mixed}}, \qquad (5)$$

where $\Delta\eta = \eta_a - \eta_b$ is the pseudorapidity separation between the particle pairs a, b, $(dN/d\Delta\phi)_{same}$ represents the normalized azimuthal distribution of particle pairs from the same event and $(dN/d\Delta\phi)_{mixed}$ represents the normalized azimuthal distribution for particle pairs in which each member is selected from different events but with a similar classification for the vertex, and centrality. The pseudorapidity requirement $|\Delta\eta| > 0.7$ was also imposed on track pairs to minimize possible non-flow contributions associated with the short-range correlations from resonance decays, Bose–Einstein correlations and jets.

The two-particle Fourier coefficients v_{nn} are obtained from the correlation function as:

$$v_{nn} = \frac{\sum_{\Delta\phi} C_r(\Delta\phi)\cos(n\Delta\phi)}{\sum_{\Delta\phi} C_r(\Delta\phi)}, \qquad (6)$$

where the $\Delta\phi$ bin width was chosen to optimize statistical significance. The v_{nn} values were then used to extract v_1^{even} via a simultaneous fit of v_{11} as a function of p_T^b for several selections of p_T^a with Eq. (3),

$$v_{11}(p_T^a, p_T^b) = v_1^{even}(p_T^a)v_1^{even}(p_T^b) - Kp_T^a p_T^b. \qquad (7)$$

Here, $K \propto 1/(\langle N_{ch}\rangle\langle p_T^2\rangle)$ takes into account the non-flow correlations induced by global momentum conservation [20,21]; $\langle N_{ch}\rangle$ is the mean multiplicity and $\langle p_T^2\rangle$ is proportional to the variance of the transverse momentum over the full phase space. The charged particle multiplicity measured in the TPC acceptance is used as a proxy for $\langle N_{ch}\rangle$. For a given centrality selection, the left hand side of Eq. (7) represents a N-by-M v_{11} matrix (i.e., N values for p_T^b for each of the M p_T^a selections) which we fit with the right hand side of Eq. (7) using $N + 1$ parameters: N values of $v_1^{even}(p_T)$ and one additional parameter K, the coefficient of momentum conservation [30]. Fig. 1 illustrates the efficacy of the fitting procedure for 0–5% central Au+Au collisions at $\sqrt{s_{NN}} = 200$ GeV. The solid curve (obtained with Eq. (7)) in each panel illustrates the effectiveness of the simultaneous fits, as well as the constraining power of the data. That is, $v_{11}(p_T^b)$ evolves from purely negative to negative and positive values as the selection range for p_T^a is increased.

The v_1^{even} extractions, were carried out for several centrality intervals at each beam energy, depending on the available statistics. The associated systematic uncertainties were estimated from variations in the extracted values after (i) varying all of the analysis cuts by a chosen range about the standard values, (ii) crosschecks to determine the uncertainty associated with the expectation that $\langle p_T v_1^{even}(p_T)\rangle \sim 0$ and (iii) varying the number of data points used in the fits. The resulting relative uncertainties, which range from $\sim 2\%$ to $\sim 10\%$, were added in quadrature to assign an overall systematic uncertainty for each measurement. The overall uncertainty for each measurement ranges from $\sim 4\%$ at $\sqrt{s_{NN}} = 200$ GeV and grows to $\sim 20\%$ at $\sqrt{s_{NN}} = 7.7$ GeV.

The resulting extracted values of $v_1^{even}(p_T)$ for 0–10% central Au+Au collisions are shown for the full span of BES-I energies in Fig. 2. These values indicate the characteristic pattern of a change from negative $v_1^{even}(p_T)$ at low p_T, to positive $v_1^{even}(p_T)$ for $p_T \gtrsim 1$ GeV/c, with a crossing point that only very slowly shifts with $\sqrt{s_{NN}}$. This predicted pattern for rapidity-even dipolar flow [19,23] is also indicated by the solid line in panel (a), which shows the result of a hydrodynamic model calculation [20]. It stems from the requirement that the net transverse momentum of the system is zero, i.e., $\langle p_T v_1^{even}(p_T)\rangle = 0$, which implies that the hydrodynamic flow direction of low-p_T particles is opposite to those for high-p_T particles. Crosschecks made with a large sample of the data, confirmed that $\langle p_T v_1^{even}(p_T)\rangle \sim 0$, within systematic uncertainties. The
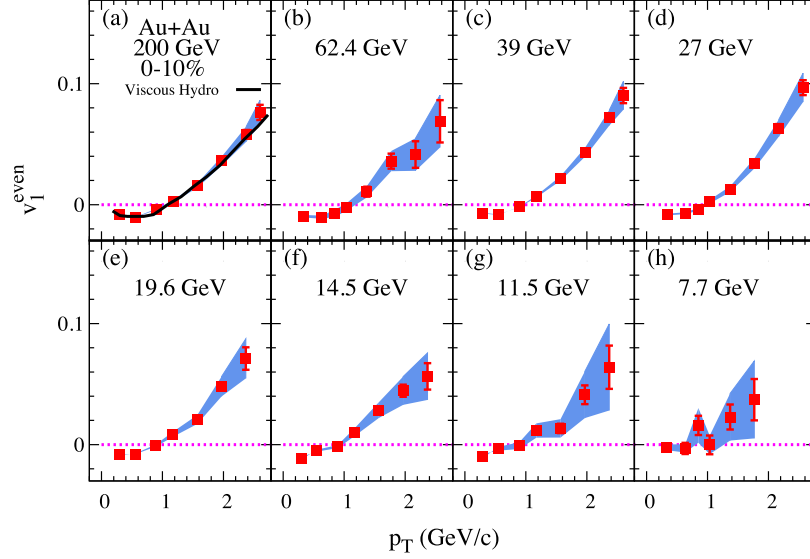
Fig. 2. Extracted values of v_1^{even} vs. p_T for 0–10% central Au+Au collisions for several values of $\sqrt{s_{NN}}$ as indicated; the v_1^{even} values are obtained via fits with Eq. (7). The curve in panel (a) shows the result from a viscous hydrodynamically based predictions [20]. The shaded bands indicate the systematic uncertainties.
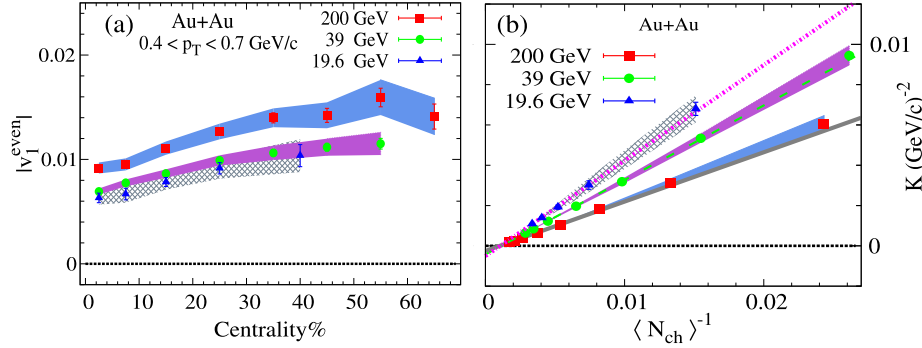

Fig. 3. (a) Centrality dependence of v_1^{even} for $0.4 < p_T < 0.7$ GeV/c for Au+Au collisions at $\sqrt{s_{NN}} = 200, 39$, and 19.6 GeV; (b) K vs. $\langle N_{ch} \rangle^{-1}$ for the v_1^{even} values shown in (a). The $\langle N_{ch} \rangle$ values correspond to the centrality intervals indicated in panel (a). The v_1^{even} and K values are obtained via fits with Eq. (7) (see text). The indicated lines show linear fits to the data; the shaded bands represent the systematic uncertainties.

crossing point is also expected to shift with $\sqrt{s_{NN}}$ since the $\langle p_T \rangle$ and $\langle p_T^2 \rangle$ values change with $\sqrt{s_{NN}}$ [30]. For these data, there is little, if any, shift due to the weak dependence of the $\langle p_T \rangle$ on $\sqrt{s_{NN}}$ for the indicated centrality selection. It is noteworthy that the low statistical significance of the data for $\sqrt{s_{NN}} < 19.6$ GeV, precluded similar centrality dependent plots for these beam energies.

The centrality dependencies of the p_T-weighted $|v_1^{even}|$ and K are shown in Figs. 3 (a) and (b) for several $\sqrt{s_{NN}}$ values as indicated, and for $0.4 < p_T < 0.7$ GeV/c; this p_T range was selected to minimize the associated statistical uncertainties and a possible influence from a change in the crossing point with $\sqrt{s_{NN}}$. For each value of $\sqrt{s_{NN}}$, Fig. 3(b) indicates a linear dependence of K on $\langle N_{ch} \rangle^{-1}$ with slopes that decrease with increasing $\sqrt{s_{NN}}$. This is to be expected since $K \propto 1/(\langle N_{ch} \rangle \langle p_T^2 \rangle)$ and the values for $\langle p_T^2 \rangle$ increase with $\sqrt{s_{NN}}$ for most of the centrality range. The increase in the magnitude of $|v_1^{even}|$ as collisions become more peripheral (Fig. 3(a)), is expected since v_1^{even} is driven by fluctuations which become more important for smaller systems, i.e., for more peripheral collisions.

Fig. 3(a) also hints at both a sizable decrease in the magnitude of $|v_1^{even}|$ and a possible weakening of its centrality dependence, as the beam energy is reduced. These patterns and the ones shown in Fig. 2 cannot be explained solely by the small change in the Glauber model eccentricity values at a given centrality which result
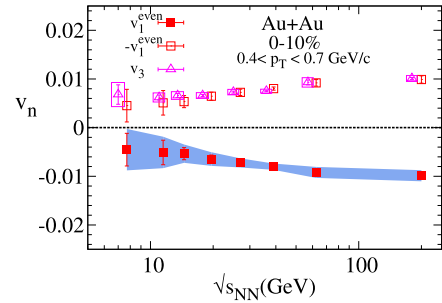

Fig. 4. Comparison of the $\sqrt{s_{NN}}$ dependence of v_1^{even} and v_3 for $0.4 < p_T < 0.7$ GeV/c in 0–10% central Au+Au collisions. The v_1^{even} results are reflected about zero (and shifted horizontally) to facilitate a comparison of the magnitudes. The shaded bands indicate the systematic uncertainties.

from a change in the beam energy. Thus, they provide a new set of supplemental constraints for the extraction of $\frac{\eta}{s}(T)$.

The constraining power of v_1^{even} is further illustrated in Fig. 4 where a comparison of the excitation functions for v_1^{even} and v_3 is shown for $0.4 < p_T < 0.7$ GeV/c; the v_1^{even} data are reflected about zero to facilitate a comparison of the magnitudes. The v_3 data, which are obtained from the present analysis, are in good agreement with the data reported in Ref. [31] for the same centrality and p_T cuts. The comparison indicates strikingly similar

magnitudes and trends for $|v_1^{even}|$ and v_3, suggesting a much larger viscous attenuation of v_3. Note that while ε_1 and ε_3 are both fluctuations-driven, $\varepsilon_3 \sim 2\varepsilon_1$ for 0–10% central Au+Au collisions [23,32] over the $\sqrt{s_{NN}}$ range of interest. A similar pattern was observed for comparisons made at higher p_T, albeit with lower statistical significance. These excitation functions are expected to provide important experimental input to ongoing theoretical attempts to pin down initial state models and make precision extractions of the specific shear viscosity.

In summary, we have employed two-particle correlation functions to carry out new measurements of the p_T and centrality dependence of the anisotropic flow coefficient v_1^{even} in Au+Au collisions spanning the beam energy range $\sqrt{s_{NN}} = 7.7$–200 GeV. The results show the expected patterns for momentum conservation and the characteristic pattern of an evolution from negative $v_1^{even}(p_T)$ for $p_T \lesssim 1$ GeV/c, to positive $v_1^{even}(p_T)$ for $p_T \gtrsim 1$ GeV/c. That is, the trends expected when initial-state geometric fluctuations act in concert with hydrodynamic-like expansion to generate rapidity-even dipolar flow. The measured dependencies on $\sqrt{s_{NN}}$, centrality and p_T, as well as the similarity in magnitude and trend of the excitation functions for v_1^{even} and v_3, constitute a new set of experimental constraints. These new constraints could prove invaluable to future theoretical attempts to discern between different initial-state models, as well as for precision extraction of the temperature dependence of the specific shear viscosity.

Acknowledgements

References

[1] D. Teaney, The effects of viscosity on spectra, elliptic flow, and HBT radii, Phys. Rev. C 68 (2003) 034913, https://doi.org/10.1103/PhysRevC.68.034913, arXiv:nucl-th/0301099.

[2] R.A. Lacey, A. Taranenko, What do elliptic flow measurements tell us about the matter created in the little bang at RHIC?, PoS CFRNC 2006 (2006) 021, arXiv:nucl-ex/0610029.

[3] P. Romatschke, U. Romatschke, Viscosity information from relativistic nuclear collisions: how perfect is the fluid observed at RHIC?, Phys. Rev. Lett. 99 (2007) 172301, https://doi.org/10.1103/PhysRevLett.99.172301, arXiv:0706.1522.

[4] B. Schenke, S. Jeon, C. Gale, Anisotropic flow in $\sqrt{s} = 2.76$ TeV Pb+Pb collisions at the LHC, Phys. Lett. B 702 (2011) 59–63, https://doi.org/10.1016/j.physletb.2011.06.065, arXiv:1102.0575.

[5] H. Song, S.A. Bass, U. Heinz, Elliptic flow in 200 A GeV Au+Au collisions and 2.76 A TeV Pb+Pb collisions: insights from viscous hydrodynamics + hadron cascade hybrid model, Phys. Rev. C 83 (2011) 054912, https://doi.org/10.1103/PhysRevC.83.054912, arXiv:1103.2380.

[6] C. Shen, U. Heinz, P. Huovinen, H. Song, Systematic parameter study of hadron spectra and elliptic flow from viscous hydrodynamic simulations of Au+Au collisions at $\sqrt{s_{NN}} = 200$ GeV, Phys. Rev. C 82 (2010) 054904, https://doi.org/10.1103/PhysRevC.82.054904, arXiv:1010.1856.

[7] F.G. Gardim, F. Grassi, M. Luzum, J.-Y. Ollitrault, Anisotropic flow in event-by-event ideal hydrodynamic simulations of $\sqrt{s_{NN}} = 200$ GeV Au+Au collisions, Phys. Rev. Lett. 109 (2012) 202302, https://doi.org/10.1103/PhysRevLett.109.202302, arXiv:1203.2882.

[8] H. Niemi, G. Denicol, P. Huovinen, E. Molnar, D. Rischke, Influence of a temperature-dependent shear viscosity on the azimuthal asymmetries of transverse momentum spectra in ultrarelativistic heavy-ion collisions, Phys. Rev. C 86 (2012) 014909, https://doi.org/10.1103/PhysRevC.86.014909, arXiv:1203.2452.

[9] G.-Y. Qin, H. Petersen, S.A. Bass, B. Muller, Translation of collision geometry fluctuations into momentum anisotropies in relativistic heavy-ion collisions, Phys. Rev. C 82 (2010) 064903, https://doi.org/10.1103/PhysRevC.82.064903, arXiv:1009.1847.

[10] B. Alver, G. Roland, Collision geometry fluctuations and triangular flow in heavy-ion collisions, Phys. Rev. C 81 (2010) 054905, Erratum: Phys. Rev. C 82 (2010) 039903, https://doi.org/10.1103/PhysRevC.82.039903, arXiv:1003.0194.

[11] B. Schenke, S. Jeon, C. Gale, Elliptic and triangular flow in event-by-event $(3 + 1)$D viscous hydrodynamics, Phys. Rev. Lett. 106 (2011) 042301, https://doi.org/10.1103/PhysRevLett.106.042301, arXiv:1009.3244.

[12] R.A. Lacey, D. Reynolds, A. Taranenko, N.N. Ajitanand, J.M. Alexander, F.-H. Liu, Y. Gu, A. Mwai, Acoustic scaling of anisotropic flow in shape-engineered events: implications for extraction of the specific shear viscosity of the quark gluon plasma, J. Phys. G 43 (10) (2016) 10LT01, https://doi.org/10.1088/0954-3899/43/10/10LT01, arXiv:1311.1728.

[13] S. McDonald, C. Shen, F. Fillion-Gourdeau, S. Jeon, C. Gale, Hydrodynamic predictions for Pb+Pb collisions at 5.02 TeV, Phys. Rev. C 95 (6) (2017) 064913, https://doi.org/10.1103/PhysRevC.95.064913, arXiv:1609.02958.

[14] J.E. Bernhard, J.S. Moreland, S.A. Bass, J. Liu, U. Heinz, Applying Bayesian parameter estimation to relativistic heavy-ion collisions: simultaneous characterization of the initial state and quark–gluon plasma medium, arXiv:1605.03954.

[15] J.-Y. Ollitrault, F.G. Gardim, Hydro overview, Nucl. Phys. A 904–905 (2013) 75c–82c, https://doi.org/10.1016/j.nuclphysa.2013.01.047, arXiv:1210.8345.

[16] A.M. Poskanzer, S.A. Voloshin, Methods for analyzing anisotropic flow in relativistic nuclear collisions, Phys. Rev. C 58 (1998) 1671–1678, https://doi.org/10.1103/PhysRevC.58.1671, arXiv:nucl-ex/9805001.

[17] R.A. Lacey, The role of elliptic flow correlations in the discovery of the sQGP at RHIC, Nucl. Phys. A 774 (2006) 199–214, https://doi.org/10.1016/j.nuclphysa.2006.06.041, arXiv:nucl-ex/0510029.

[18] N. Borghini, P.M. Dinh, J.-Y. Ollitrault, Are flow measurements at SPS reliable?, Phys. Rev. C 62 (2000) 034902, https://doi.org/10.1103/PhysRevC.62.034902, arXiv:nucl-th/0004026.

[19] M. Luzum, J.-Y. Ollitrault, Directed flow at midrapidity in heavy-ion collisions, Phys. Rev. Lett. 106 (2011) 102301, https://doi.org/10.1103/PhysRevLett.106.102301, arXiv:1011.6361.

[20] E. Retinskaya, M. Luzum, J.-Y. Ollitrault, Directed flow at midrapidity in $\sqrt{s_{NN}} = 2.76$ TeV Pb+Pb collisions, Phys. Rev. Lett. 108 (2012) 252302, https://doi.org/10.1103/PhysRevLett.108.252302, arXiv:1203.0931.

[21] G. Aad, et al., Measurement of the azimuthal anisotropy for charged particle production in $\sqrt{s_{NN}} = 2.76$ TeV lead–lead collisions with the ATLAS detector, Phys. Rev. C 86 (2012) 014907, https://doi.org/10.1103/PhysRevC.86.014907, arXiv:1203.3087.

[22] P. Danielewicz, R. Lacey, W.G. Lynch, Determination of the equation of state of dense matter, Science 298 (2002) 1592–1596, https://doi.org/10.1126/science.1078070, arXiv:nucl-th/0208016.

[23] D. Teaney, L. Yan, Triangularity and dipole asymmetry in heavy ion collisions, Phys. Rev. C 83 (2011) 064904, https://doi.org/10.1103/PhysRevC.83.064904, arXiv:1010.1876.

[24] F.G. Gardim, F. Grassi, Y. Hama, M. Luzum, J.-Y. Ollitrault, Directed flow at mid-rapidity in event-by-event hydrodynamics, Phys. Rev. C 83 (2011) 064901, https://doi.org/10.1103/PhysRevC.83.064901, arXiv:1103.4605.

[25] R.A. Lacey, Indications for a critical end point in the phase diagram for hot and dense nuclear matter, Phys. Rev. Lett. 114 (14) (2015) 142301, https://doi.org/10.1103/PhysRevLett.114.142301, arXiv:1411.7931.

[26] N. Borghini, P.M. Dinh, J.-Y. Ollitrault, A.M. Poskanzer, S.A. Voloshin, Effects of momentum conservation on the analysis of anisotropic flow, Phys. Rev. C 66 (2002) 014901, https://doi.org/10.1103/PhysRevC.66.014901, arXiv:nucl-th/0202013.

[27] M. Anderson, et al., The STAR time projection chamber: a unique tool for studying high multiplicity events at RHIC, Nucl. Instrum. Methods A 499 (2003) 659–678, https://doi.org/10.1016/S0168-9002(02)01964-2, arXiv:nucl-ex/0301015.

[28] L. Adamczyk, et al., Inclusive charged hadron elliptic flow in Au+Au collisions at $\sqrt{s_{NN}} = 7.7$–39 GeV, Phys. Rev. C 86 (2012) 054908, https://doi.org/10.1103/PhysRevC.86.054908, arXiv:1206.5528.

[29] B.I. Abelev, et al., Identified particle production, azimuthal anisotropy, and interferometry measurements in Au + Au collisions at $\sqrt{s_{NN}} = 9.2$ GeV, Phys. Rev. C 81 (2010) 024911, https://doi.org/10.1103/PhysRevC.81.024911, arXiv:0909.4131.

[30] J. Jia, S.K. Radhakrishnan, S. Mohapatra, A study of the anisotropy associated with dipole asymmetry in heavy ion collisions, J. Phys. G 40 (2013) 105108, https://doi.org/10.1088/0954-3899/40/10/105108, arXiv:1203.3410.

[31] L. Adamczyk, et al., Beam energy dependence of the third harmonic of azimuthal correlations in Au+Au collisions at RHIC, Phys. Rev. Lett. 116 (11) (2016) 112302, https://doi.org/10.1103/PhysRevLett.116.112302, arXiv:1601.01999.

[32] P. Bozek, Event-by-event viscous hydrodynamics for Cu–Au collisions at $\sqrt{s_{NN}} = 200$ GeV, Phys. Lett. B 717 (2012) 287–290, https://doi.org/10.1016/j.physletb.2012.09.040, arXiv:1208.1887.